Method of accurately calculating mean field operator in multi-configuration time-dependent Hartree–Fock frame*

Li Wen-Liang(李文亮)†, Zhang Ji(张 季), and Yao Hong-Bin(姚洪斌)

Xinjiang Institute of Engineering, Xinjiang 830091, *China*

(Received 14 December 2012; revised manuscript received 27 March 2013)

The accurate theoretical expressions of the mean field operator associated with the multi-configuration time-dependent Hartree–Fock (MCTDHF) method are presented in this paper. By using a theoretical formula, derived without approximation, we can study the multi-electron correlation dynamics accurately. Some illustrative calculations are carried out to check the accuracy of the expression of the mean field operator. The results of illustrative calculations indicate the reliability of the accurate expression of the mean field operator. This theoretical calculation method for the mean field operator may be of considerable help in future studies of the correlated dynamics of many-electron systems in strong laser fields.

Keywords: strong laser field, multi-electron dynamics, mean field operator

PACS: 32.80.Rm, 42.65.Ky, 42.65.Re **DOI:** 10.1088/1674-1056/22/9/093202

1. Introduction

In recent years, there has been increasing interest in the correlated dynamics of many-electron systems.[1–5] Theorists have developed a variety of explicit time-dependent electronic structural methods, and experimentalists are now able to analyze and control the dynamics of electrons with sub-femtosecond resolution. An important method known as the multi-configuration time-dependent Hartree (MCTDH) method has been developed.[6–17] In 2003, Zanghellini *et al.*[6] developed the MCTDHF method to deal with multi-electron dynamics in strong laser fields. Then, Zanghellini *et al.*[7] made further calculations using the MCTDHF method. Caillat *et al.*[8] showed that the method provides a good approximation of time-dependent multi-electron wave-functions and can deal with the correlation of multi-electron systems in strong laser fields. Kato and Kono,[9] and Kato and Yamanouchi[10] developed the theory in the second-quantization formalism. Nest *et al.*,[11] Nest and Klamroth,[12] and Nest[13,14] further developed the MCTDHF method by using atomic basis functions, following which, Nest *et al.*[15] studied the electronically excited states of molecules, and Remacle *et al.*[17] and Nest *et al.*[18] investigated the ultrafast electron dynamics in LiH. The principle difference between the two versions is the difference in the type of basis function. In Refs. [11]– [14], atomic basis functions were used, but in Refs. [6]–[8] the grid vectors were adopted as the basis functions. The difference in the type of basis function will result in a different construction method for the necessary matrix elements of the operators in the MCTDHF calculation.

The accurate study of the correlation dynamics of multi-electron systems in a strong laser field requires accurate expressions of the mean field part in the MCTDHF working equations. However, some approximations were used in previous versions to deal with the mean field operator. In order to develop an accurate method of handling the electron-electron potential, a new set of equations is derived and the formula for the mean field operator is derived without approximation.

The rest of the present paper is organized as follows. In Section 2, the theory of the MCTDHF with a special focus on the derivation of the mean field part is briefly described. In Section 3, the helium atom and the hydrogen molecule are calculated as an example. The working equations are propagated in imaginary time, and the ground state energy is obtained. The intensity and time dependence of the multiphoton ionization of helium in a strong laser field are also presented. In Section 4, some conclusions are drawn from the present study. Atomic units are used throughout the paper, unless otherwise stated.

2. Theory

In this section, we will present an outline of the MCTDHF method, with special focus on an accurate derivation of the formula for the mean field operator. Our notation follows closely the standard notations of the MCTDH method for nuclear quantum dynamics[19–21] and those presented by Nest *et al.*[11–14]

In the MCTDHF method, the N-electron wave function can be linearly combined into a time-dependent Slater deter-

*Project supported by the Scientific Research Program of the Higher Education Institution of Xinjiang, China (Grant No. XJEDU2012S41) and the National Natural Science Foundation of China (Grant No. 10974198).

†Corresponding author. E-mail: wenliangli.dicp@gmail.com

© 2013 Chinese Physical Society and IOP Publishing Ltd

minant as follows:

$$\Psi(\boldsymbol{x}_1,\boldsymbol{x}_2,\ldots\boldsymbol{x}_N,t) = \frac{1}{\sqrt{N!}}\sum_J A_J(t)|\chi_{j_1}(\boldsymbol{x}_1,t)\ldots\chi_{j_N}(\boldsymbol{x}_N,t)| = \frac{1}{\sqrt{N!}}\sum_J A_J(t)|J,t\rangle. \quad (1)$$

The coefficient tensor A_J and the spin–orbital $\chi_{j_1}(\boldsymbol{x}_1,t)$ are time-dependent. The capital letter J is a composite index which enumerates the spin–orbital number appearing in the determinant, and $\boldsymbol{x}_i = (\boldsymbol{r}_i, s_i)$ is a composite variable for the position $\boldsymbol{r}_i$ and the spin coordinate s_i. To visualize the equation, we take a system of 2 electrons with 4 spin orbitals

$$\Psi(\boldsymbol{x}_1,\boldsymbol{x}_2t) = \frac{1}{\sqrt{2!}}\{A_{(1,2)}|\chi_1\chi_2\rangle + A_{(1,3)}|\chi_1\chi_3\rangle + A_{(1,4)}|\chi_1\chi_4\rangle + A_{(2,3)}|\chi_2,\chi_3\rangle + A_{(2,4)}|\chi_2,\chi_4\rangle + A_{(3,4)}|\chi_3,\chi_4\rangle\}. \quad (2)$$

In the above equation, the linear coefficient A_J and the spin orbital are all assumed to be time-dependent, $|\chi_1\chi_2\rangle$, etc. are the Slater determinants which can be expressed as linear combinations of Hartree products.

The Hamiltonian describing the N-electron system which interacts with the strong laser field can be expressed as follows:

$$H = \sum_{i=1}^{N}\frac{p_i^2}{2} + \sum_{i=1}^{N}[V(r_i)] + \sum_{i}^{N}\sum_{i>j}^{N}\frac{1}{r_{ij}}. \quad (3)$$

Here, the external potential $V(r_i)$ is produced by the (fixed) nucleus potential $V_{\rm nuc}(r_i)$ and may also contain the coupling to an additional laser field in the dipole approximation $V_{\rm external}(r_i)$. Then, by using the variational principle with respect to the coefficients and spin orbitals, respectively

$$\left\langle \delta\Psi(t)\,\middle|\, H - \mathrm{i}\frac{\partial}{\partial t}\,\middle|\,\Psi(t)\right\rangle = 0, \quad (4)$$

the corresponding equations of motion A_J and $\chi_{j_1}(x_1,t)$ are found to be

$$\mathrm{i}\frac{\mathrm{d}A_J}{\mathrm{d}t} = \frac{1}{N!}\sum_L\langle J|H|L\rangle A_L, \quad (5)$$

$$\mathrm{i}\frac{\mathrm{d}\chi}{\mathrm{d}t} = (1-P)\rho^{-1}\langle H\rangle\chi, \quad (6)$$

where P is the projector operator in the space spanned by the single particle functions, $P = \sum_i|\chi_i\rangle\langle\chi_i|$; ρ is the density operator and

$$\rho_{ij} = \left\langle\frac{\partial\Psi}{\partial\chi_i}\,\middle|\,\frac{\partial\Psi}{\partial\chi_j}\right\rangle,$$

$\langle H\rangle$ is the so-called mean field operator

$$\langle H\rangle_{ij} = \left\langle\frac{\partial\Psi}{\partial\chi_i}\,\middle|\,H\,\middle|\,\frac{\partial\Psi}{\partial\chi_j}\right\rangle.$$

In order to solve Eqs. (4) and (5), we can use grid basis functions as used in Refs. [6]–[8], or atomic basis functionsin Refs. [11]–[14]. In the process of our derivation of the working equation and in our source code, the basis functions in the calculation are atomic basis functions ξ_k, in other words, the space orbital ϕ_i is combined with atomic orbitals, $\phi_i = \sum_k C_{i,k}\xi_k$, and the spin orbital is as follows:

$$\chi_i = \phi_i^* s_i = s_i^*\sum_k C_{i,k}\xi_k. \quad (7)$$

We then write Eq. (4) as an algebraic expression

$$\mathrm{i}\begin{pmatrix}\frac{\mathrm{d}A_1}{\mathrm{d}t}\\ \frac{\mathrm{d}A_2}{\mathrm{d}t}\\ \frac{\mathrm{d}A_3}{\mathrm{d}t}\\ \cdots\end{pmatrix} = \frac{1}{N!}\begin{pmatrix}\langle J_1|H|J_1\rangle & \langle J_1|H|J_2\rangle & \langle J_1|H|J_3\rangle & \ldots\\ \langle J_2|H|J_1\rangle & \langle J_2|H|J_2\rangle & \langle J_2|H|J_2\rangle & \ldots\\ \langle J_2|H|J_1\rangle & \langle J_2|H|J_2\rangle & \langle J_2|H|J_2\rangle & \ldots\\ \cdots & \cdots & \cdots & \cdots\end{pmatrix}\begin{pmatrix}A_1\\ A_2\\ A_3\\ \cdots\end{pmatrix}. \quad (8)$$

Each element of the algebraic equation can be solved by the Slater rules[22] and then the differential algebraic equation can be solved numerically.

In the same way, we can obtain the algebraic form of Eq. (6). We will deduce the equation in a general way. The element of the mean field operator is

$$\langle H\rangle_{ij} = \left\langle\frac{\partial\Psi}{\partial\chi_i}\,\middle|\,H\,\middle|\,\frac{\partial\Psi}{\partial\chi_j}\right\rangle,$$

and $|\partial\Psi/\partial\chi_j\rangle$ is a single-hole function, which is the derivative of the system wave-function Ψ, which can be solved by Eq. (1). We assume that electron 1 is missed, following the nuclear dynamics method of Refs. [19]–[21]. After the derivation and reformulation, it is found that the single hole function is also a combination of Slater determinants, in which the coordinates of electron 1 are absent. We assume that the numbers of the spin orbitals used in calculation is equal to the value number.

$$\left|\frac{\partial\Psi}{\partial\chi_j}\right\rangle = \sum_M A_M|M\rangle. \quad (9)$$

It is important to emphasize again that there are only number-1 spin orbitals in the Slater $|M\rangle$ and the coordinates of the missed electron 1 are absent.

Inserting Eq. (9) into the expression for the element of the mean field operator

$$\left\langle\frac{\partial\Psi}{\partial\chi_i}\,\middle|\,H\,\middle|\,\frac{\partial\Psi}{\partial\chi_j}\right\rangle,$$

we obtain

$$\left\langle\frac{\partial\Psi}{\partial\chi_i}\,\middle|\,H\,\middle|\,\frac{\partial\Psi}{\partial\chi_j}\right\rangle = \sum_M\sum_L A_M A_N\langle M|H|L\rangle. \quad (10)$$

As we emphasize above, the Slater $|M\rangle$ and $|L\rangle$ do not contain the coordinates of the missing electron 1, so we can decompose the Hamiltonian of this system into four parts

$$H(r_1,r_2,r_3,\ldots) = h(r_1) + \sum_1\sum_{i>1}\frac{1}{r_{1i}} + \sum_i h(r_i) + \sum_{i>1}\sum_{j>i}\frac{1}{r_{ij}}. \quad (11)$$

On the right-hand side of Eq. (11), the first part is the single electron Hamiltonian term of electron 1, the second part is the

coulomb interaction between electron 1 and all other electrons the third part and the fourth part do not contain the coordinates of electron 1 and will not contribute to the calculation after a projection which only contains the coordinates of electron 1.

Inserting Eq. (11) into Eq. (10), we obtain elements of the mean field operator as

$$\begin{aligned}
&\sum_M \sum_L A^*_{i,M} A_{j,N} \langle M|H|L\rangle \\
&= \sum_M \sum_L A^*_{i,M} A_{j,N} \langle M|h(r_1) + \sum_1 \sum_{i>1} \frac{1}{r_{1i}}|L\rangle \\
&= \sum_M \sum_L A^*_{i,M} A_{j,N} \langle M|h(r_1)|L\rangle \\
&\quad + (f-1)^* \sum_M \sum_L A^*_{i,M} A_{j,N} \langle M|\frac{1}{r_{12}}|L\rangle \\
&= h(r_1)\rho_{i,j} + (f-1)^* \sum_M \sum_L A^*_{i,M} A_{j,N} \langle M|\frac{1}{r_{12}}|L\rangle. \qquad (12)
\end{aligned}$$

The first part in the atomic basis functions can be expressed as

$$\rho_{i,j}\langle \xi|h(r_1)|\zeta\rangle, \qquad (13)$$

where $|\zeta\rangle$ and $|\xi\rangle$ are orthogonal atomic basis functions. The element $\langle \xi|h(r_1)|\zeta\rangle$ can be obtained from the transformation as

$$h = X^+ h^* X, \qquad (14)$$

where h^* is the element operator in the non-orthogonal atomic basis function space and X is the transform matrix between the non-orthogonal space and the orthogonal space.

To achieve an accurate derivation the second part is somewhat complicated and a detailed derivation will be presented in the following section. Since the Slater determinants $|L\rangle$ and $|M\rangle$ do not contain the coordinates of electron 1, only the spin orbital with coordinate 2 is involved

$$\sum_{j_2}\sum_{k_2}\sum_{j_3}\cdots\sum_{j_f} A^*_{i,j_2,j_3\ldots j_f} A_{j,k_2,j_3\ldots j_f} \left\langle \chi_{j_2} \left| \frac{1}{r_{12}} \right| \chi_{k_2} \right\rangle. \qquad (15)$$

The spin orbital is

$$\chi_i = \phi_i^* s_i = s_i^* \sum_k C_{i,k}\xi_k. \qquad (16)$$

Inserting Eq. (16) into Eq. (15), we obtain

$$\begin{aligned}
&\sum_{j_2}\sum_{k_2}\sum_{j_3}\cdots\sum_{j_f} A^*_{i,j_2,j_3\ldots j_f} A_{j,k_2,j_3\ldots j_f} \\
&\times \left\langle \left(\sum_k C_{j_2,k}\xi_k\right)^* \left| \frac{1}{r_{12}} \right| \left(\sum_k C_{k_2,k}\xi_k\right) \right\rangle \delta_{s_i s_j}. \qquad (17)
\end{aligned}$$

In the above expression, $\delta_{s_i s_j}$ is a Delta function. We can easily obtain the matrix element in atomic basis functions

$$\begin{aligned}
&\langle\zeta_p| \sum_{j_2}\sum_{k_2}\sum_{j_3}\cdots\sum_{j_f} A^*_{i,j_2,j_3\ldots j_f} A_{j,k_2,j_3\ldots j_f} \\
&\times \left\langle \left(\sum_k C^*_{j_2,k}\xi_k\right) \left| \frac{1}{r_{12}} \right| \left(\sum_l C_{k_2,l}\xi_l\right) \right\rangle |\xi_u\rangle \delta_{s_i,s_j} \\
&= \sum_{j_2}\sum_{k_2}\sum_{j_3}\cdots\sum_{j_f} A^*_{i,j_2,j_3\ldots j_f} A_{j,k_2,j_3\ldots j_f} \\
&\times \sum_{k\in\xi}\sum_{l\in\xi} C^*_{j_2,k} C_{k_2,l} \left\langle \xi_k\zeta_p \left| \frac{1}{r_{12}} \right| \xi_l\xi_u \right\rangle \delta_{s_i,s_j}. \qquad (18)
\end{aligned}$$

The element $\langle\xi_k\zeta_p|(1/r_{12})|\xi_l\xi_u\rangle$ in Eq. (18) is the two-electron integral in the orthogonal basis function space. First of all, we calculate the two-electron integral in the non-orthogonal atomic basis function space, then transform the integral values to the orthogonal space. Finally, using the theoretical formula (18), we can calculate the mean field operator exactly.

3. Illustrative calculation

To accurately test the correctness of the derivation of the mean field and the stability of the Fortran source code, we take a helium atom and a hydrogen molecule as typical two-electron systems. We calculate the ground state energies of helium and the hydrogen molecule by propagating the initial wave function in imaginary time in the absence of an external strong laser field.

We firstly propagate the wave function of the helium atom in imaginary time. The first calculation is performed in the basis set 6-311G. The operators that appear in the motion equations are represented in this Gauss-type function basis. For this we firstly conduct an HF calculation using the Molpro[23] or Gamess[24] program package. We can also use the Slater-type function as the basis sets, which was used in the SMILES2007 program package.[25,26] All our calculations are performed in the orthogonal basis set. For a given number of spin orbitals ($N_{\rm so}$), there are $C^N_{N_{\rm so}}$ independent determinants. We will employ the usual CASSCF notation $\begin{pmatrix} N_{\rm so} \\ N \end{pmatrix}$ to refer to a system with N electron and $N_{\rm so}/2$ spatial orbitals.

The ground energy of helium is calculated by propagating the wave function in imaginary time and the results are shown in Fig. 1. To prepare the initial wave function and the necessary matrix elements of operators, we firstly conduct a Hartree–Fock calculation. Then, the matrix elements of the necessary operators and the Hartree spatial orbitals are available. There are a variety of methods to construct the initial spin orbitals, and we illustrate two methods to achieve this goal, one of which is as follows. The matrix of the single electron Hamlitonian h is available after the HF calculation and we can initialize the spatial orbitals through diagonalization of h. Four spin orbitals are used in the calculation. Consider those four initial spin orbitals as initial wavefunctions. We can obtain the relaxation energy versus time as shown by solid curve in Fig. 1. The dash-dot line in Fig. 1 represents the result of another calculation in which the Fock operator F was diagonalized to obtain the initial spin orbitals. The Fock operator is combined with the single electron Hamlitonian h and p^*G. The G operator represents the two electron integral part, whose expression can be found from Ref. [21] and the p indicates the

Hartree–Fock density matrix, $p_{\mu\upsilon} = \sum_{ij} c^*_{i\mu} c_{j\upsilon}$. There are also four spin orbitals used in the calculation. The initial values of coefficient A_J are identical to each other. In the above methods, the values of A_J are all set to be $1/\sqrt{N}$ for $J = (1, 2, ..N)$ and zero otherwise. Though two different initial conditions are used to prepare the wave function, it is clear from Fig. 1 that the same accurate ground state energy, about -2.8755 Hartree (1 Hartree $= 110.5 \times 10^{-21}$ J), is obtained.

In order to test the influence of the number of the active space on the relaxation energy of the atom when propagating the wave function in imaginary time, we carry out the propagation by increasing the active space from a single determinant [CAS(2,1), HF], to 15 determinants [CAS(2,3)]. The results are listed in Fig. 2. The horizontal solid lines indicate $E_{\rm HF} = -2.8759$ Hartree and the other horizontal line is $E_{\rm FCI} = -2.876418$ Hartree (energy of full configuration interaction). $E_{\rm HF}$ and $E_{\rm FCI}$ are calculated using the Molpro *ab initio* program package[23] at the same basis set level.

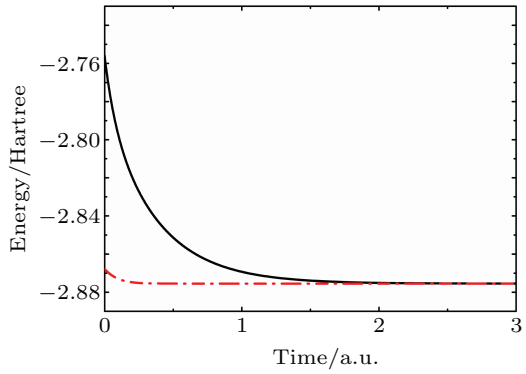


Fig. 1. (color online) Energy expectation values for different initial conditions for the propagation in imaginary time. The solid line represents the initial condition which was diagonalized from the single electron Hamlitonian h. The dash–dot line shows diagonalization from the Fock operator. The atomic basis set is 6-311G.

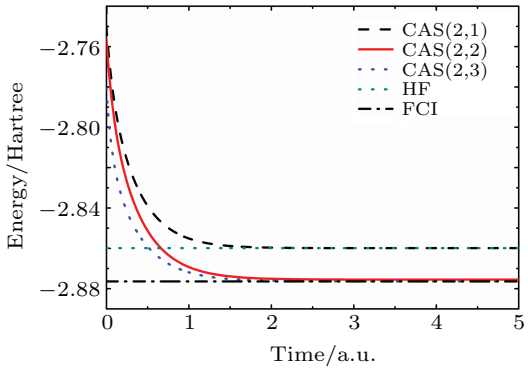


Fig. 2. (color online) Energy relaxation during propagation in imaginary time for the helium atom. The active space is increased from a single determinant CAS(2,1) (dash line), to 15 determinants CAS(2,3) (dot line). The values of $E_{\rm HF} = -2.8759$ Hartree (straight dot line) and $E_{\rm FCI} = -2.876418$ Hartree (dash–dot line) is calculated by MOLPRO. The relaxation energy of [CAS(2,1), HF] in our calculation is -2.8755 Hartree. The relaxation energy of [CAS(2,3)] in our calculation is -2.87642 Hartree. The atomic basis set is 6-311G.

All the initial spin orbitals are achieved by diagonalizing the single electron Hamlitonian. The initial guessed energy is much larger than the HF energy. This figure shows how the final energies include more and more correlation energy, as the number of orbitals increases. It is very clear that the energy calculated by propagating the (2, 1) MCTDHF wave-function in imaginary time reproduces the HF ground state energy perfectly. The energy of (2, 1) is -2.8755 Hartree. When the spin orbital number increases, the energy becomes much closer to the FCI energy. The dashed line is the result of (2, 3), and produces the energy -2.87642 Hartree which is much closer to the FCI energy -2.87618 Hartree calculated by MOLPRO.[23]

Next, we turn our attention to the hydrogen molecule. In the calculation of the hydrogen molecule, the basis set is vdz. For a simple test, the inter-nuclear distance is assumed to be fixed at the equilibrium geometry. The initial A_J are set to be $1/\sqrt{N_{\rm combin}}$ for all possible Slater determinants. The $N_{\rm combin}$ is the number of Slater determinants. The results are shown in Fig. 3. The left panel of Fig. 3 is the result of CAS (2, 1) and CAS (2, 2) by propagating the initial wave function in imaginary time. The dash–dot line in the left panel is the HF energy of hydrogen in the ground state, about -2.84255 Hartree, which is calculated by MOLPRO using the same basis. It is clear that the energy which is propagated by MCTDHF-CAS (2, 1) method relaxes to almost the same energy -2.84256 Hartree. When we increase the active space to CAS (2, 2), we obtain a value of the relaxation energy closer to the FCI energy.

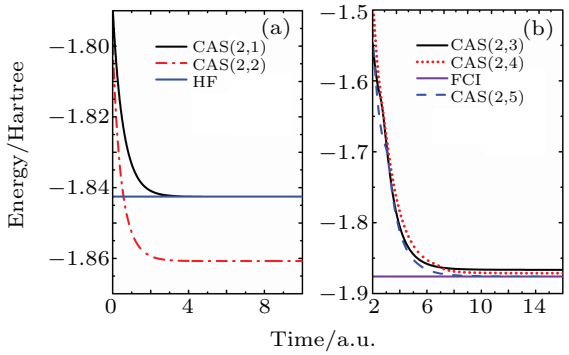


Fig. 3. (color online) Energy relaxation during propagation in imaginary time for the hydrogen molecule. The active space is increased from a single determinant CAS(2,1) (solid line) to CAS(2,2) (dash-dot line) in the left panel. The line in the left panel (a) shows the HF energy calculated by MOLPRO. The active spaces are CAS(2,3) (solid line), CAS(2,4) (dotted line) and CAS(2,5) (dashed line) in the right panel (b). The straight solid line in the right panel shows the FCI energy calculated by MOLPRO. The difference between the most accurate MCTDHF calculation and the FCI result is less than 0.1 kcal/mol. The atomic basis set is vdz.

To test the influence of the number of the active spaces on the relaxation energy of the molecule when propagating the wavefunction in imaginary time, we increase the active space to CAS (2, 3), CAS (2, 4), CAS (2, 5), and show the results in the right panel of Fig. 3. When the number of active spaces is increased, the energy which is relaxed by MCTDHF method in imaginary time becomes closer and closer to the FCI energy of

the hydrogen molecule. The difference between the most accurate MCTDHF calculation and the FCI energy is less than 0.1 kcal/mol.

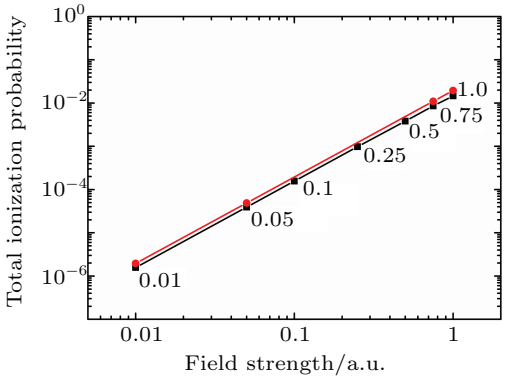


Fig. 4. (color online) Total ionization probability of helium versus electric field strength (in atomic units) for 6-cycle laser pulse with $\hbar\omega = 136$ eV ($\omega = 5$ a.u.). The solid circles denote the results of (5+1)-dimensional time-dependent Schrödinger equation (TDSE), and the squares denote the present results obtained using the MCTDHF method.

Using the propagation in imaginary time method, the atomic or molecular ground state wave function can be accurately determined. When accurate ground state wave functions are achieved, we can further investigate the interaction between a laser pulse and a helium atom. In our calculations, the atomic basis set is 6-311G (2df, 2pd), which comprises 14 Cartesian atomic orbitals. We choose 12 spin orbitals for the 2-active-electron system which give rise to 66 singlet determinants. Figure 4 shows the total ionization probability versus electric field strength ε for a 6-cycle laser pulse with $\sin^2$ temporal shape and central frequency $\omega = 5$ a.u. (atomic units) as shown in Fig. 5. This set of parameters and pulse shape have been chosen so as to match those employed in a calculation by Birkeland *et al.*[27] The probability of finding two electrons in bound states is expressed as[28,29]

$$\sum_{j_1,j_2} P_{j_1,j_2} = \sum_{j_1,j_2} |\langle \chi_{j_1}\chi_{j_2}|\Psi(\boldsymbol{x}_1,\boldsymbol{x}_2,t)\rangle|.$$

Then we obtain the total ionization probability

$$P^{\text{tot}} = 1 - \sum_{j_1,j_2} P_{j_1,j_2}.$$

By comparing with the results of $(5+1)$-dimensional time-dependent Schrödinger equation (TDSE),[27] the total ionization probability as a function of intensity of laser field, obtained using the MCTDHF method, is in good agreement with the theoretical prediction in Ref. [21], which indicates that our derivation of the mean field operator is very correct. In order to obtain more information about the process of ionization, we present the results of time evolution of total ionization probability at six different electronic field strengths ($\varepsilon = 0.01$ a.u., 0.05 a.u., 0.1 a.u., 0.25 a.u., 0.5 a.u., 1 a.u.) as shown in Fig. 6. The two panels in Fig. 6 show that the time dependences of ionization probabilities present obvious oscillations and reach maximum or minimum simultaneously because of the "rescattering" of the wave packets driven back by the laser pulse with $\sin^2$ temporal shape.[30] We can also find that the total ionization probabilities follow the field variation, but with a doubled frequency because both positive and negative oscillations of the field interact with electrons in the same way. Now we turn to the right panel of Fig. 6, which is plotted on linear scales, we can clearly find that the oscillations of the time dependences of ionization probabilities become increasingly strong with the increment of electronic field strength.

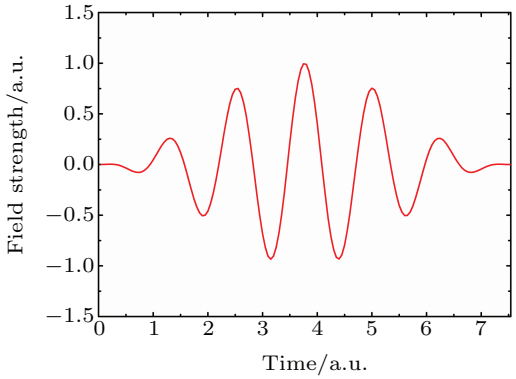


Fig. 5. (color online) Concerned 6-cycle laser pulse with a $\sin^2$ envelope with a photon energy of $\hbar\omega = 136$ eV and a peak strength of $\varepsilon = 1$ a.u.

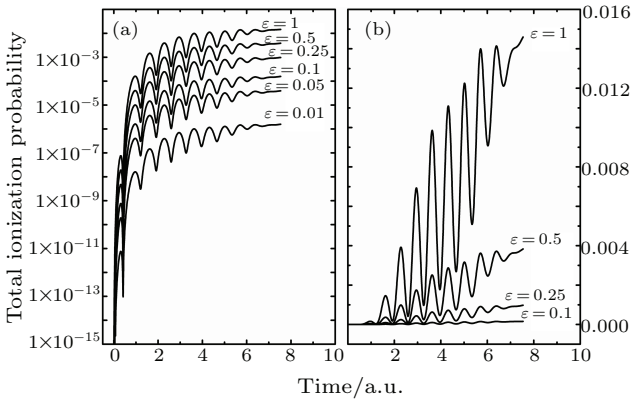


Fig. 6. Results of the time evolution of total ionization probability at six different electronic field strengths ($\varepsilon = 0.01$ a.u., 0.05 a.u., 0.1 a.u., 0.25 a.u., 0.5 a.u., 1 a.u.), the left panel (a) is plotted on logarithmic scales, and the right panel (b) is plotted on linear scales.

We also calculate the time dependences of the electronic ground-state population, average energy and dipole moment during the pulse interaction in order to trace the dynamic behavior of the field-atom interaction in great detail. The probability for helium atom being in the ground state is estimated by $P^0 = |\langle \Psi(\boldsymbol{x}_1,\boldsymbol{x}_2,0)|\Psi(\boldsymbol{x}_1,\boldsymbol{x}_2,t)\rangle|$. The results of time dependences of the electronic ground-state population (left panel) and average energy (right panel) are shown in Fig. 7 at four different electronic field strengths ($\varepsilon = 0.01$ a.u., 0.5 a.u., 0.75 a.u., 1 a.u.). As can be seen from Fig. 7, the electronic ground-state population and average energies oscillate with a doubled frequency synchronously with the electric field and

the oscillations become increasingly strong with the increment of the field, which is highly consistent with Fig. 6. The ground state population shown in the left panel of Fig. 7 is depleted most effectively when the electronic laser field is at maximum amplitude. The continuously dropping population peaks indicate that the returning wave packets scatter mostly away from the ground state. In contrast, when the field becomes weak the population peaks gradually become higher because the returning wave packets driven by the field are recombined into the ground state.[30] Finally, we investigate the dipole moments in the direction of the field at three different intensities ($\varepsilon =$ 0.5 a.u., 0.75 a.u., 1 a.u.) in Fig. 8. The dipole moment can be expressed as $\mu(t) = \langle \Psi(\boldsymbol{x}_1, \boldsymbol{x}_2, t)|\boldsymbol{r}|\Psi(\boldsymbol{x}_1, \boldsymbol{x}_2, t)\rangle$, where r denotes the distance between an electron and the nucleus. Actually $\mu(t)$ means the time evolution of the average distance from an electron to the nucleus. As the intensity increases, the oscillations of $\mu(t)$ with the same frequency as laser pulse frequency become increasingly strong, indicating the higher intensity considerably facilitates electrons moving far from nucleus.

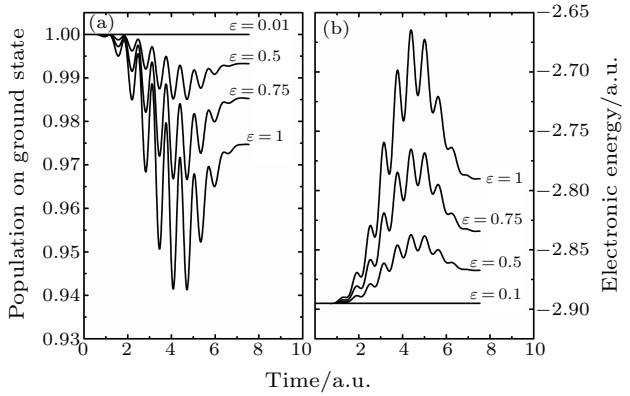


Fig. 7. Results of time dependence of the electronic ground-state population (left panel (a)) and average energy (right panel (b)) at four different electronic field strengths ($\varepsilon = 0.01$ a.u., 0.5 a.u., 0.75 a.u., 1 a.u.).

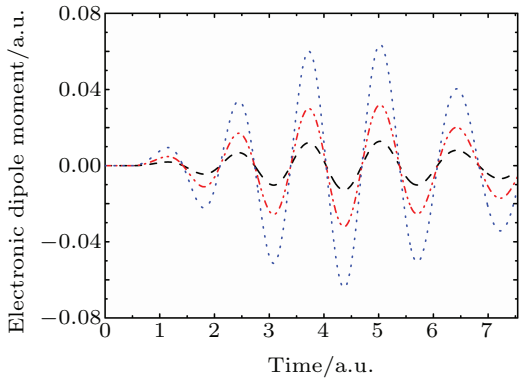


Fig. 8. (color online) Results of dipole moments in the direction of the field at three different intensities, $\varepsilon = 0.1$ a.u. (dash line), $\varepsilon = 0.25$ a.u. (dash-dot line), $\varepsilon = 0.5$ a.u. (dot line).

4. Conclusion

A new theoretical method to deduce an accurate formula of the mean field operator is presented. Some illustrative calculations are carried out to check the accuracy of the expression of the mean field operator. The calculated results indicate high confidence in the accurate theoretical formula of the mean field operator. The strict theoretical expression of the mean field operator may be a great help for studying the correlated dynamics of many-electron system in a strong laser field.

5. Acknowledgment

We are indebted to Dr. Xu Wen-Wu (who is working at the Shanghai Institute of Applied Physics, Chinese Academy of Sciences) for the many helpful discussions, writing the ionization analysis modules, and conducting the calculation. Zhang Ji is also the first author. Li has derived the formulas and written the MPI parallel calculation source code.

References

[1] Hu S L and Shi T Y 2013 *Chin. Phys. B* **22** 013101
[2] Yu B H, Li Y B and Tang Q B 2013 *Chin. Phys. B* **22** 013206
[3] Song Y D, Chen Z, Sun C K and Hu Z 2013 *Chin. Phys. B* **22** 013302
[4] Jia X Y, Fan D H, Li W D and Chen J 2013 *Chin. Phys. B* **22** 013303
[5] Guo F M, Chen G, Chen J G, Li S Y and Yang Y J 2013 *Chin. Phys. B* **22** 023204
[6] Zanghellini J, Kitzler M, Fabian C, Brabec T and Scrinzi A 2003 *Laser Phys.* **13** 1064
[7] Zanghellini J, Kitzler M, Brabec T and Scrnzi A 2004 *J. Phys. B: At. Mol. Opt. Phys.* **37** 763
[8] Caillat J, Zhanghellini J, Kitzler M, Koch O, Kreuzer W and Scrinzi A 2005 *Phys. Rev. A* **71** 012712
[9] Kato T and Kono H 2004 *Chem. Phys. Lett.* **392** 533
[10] Kato T and Yamanouchi K 2009 *J. Chem. Phys.* **131** 164118
[11] Nest M, Klamroth T and Saalfrank P 2005 *J. Chem. Phys.* **122** 124102
[12] Nest M and Klamroth T 2005 *Phys. Rev. A* **72** 012710
[13] Nest M 2007 *J. Theor. Comput. Chem.* **6** 563
[14] Nest M 2009 *J. Chem. Phys.* **472** 171
[15] Nest M, Padmanaban R and Saalfrank P 2007 *J. Chem. Phys.* **126** 124106
[16] Haxton D J, Lawler K V and McCurdy C M 2011 *Phys. Rev. A* **83** 063416
[17] Remacle F, Nest M and Levine R D 2007 *Phys. Rev. Lett.* **99** 183902
[18] Nest M, Remacle F and Levine R D 2008 *New J. Phys.* **10** 025019
[19] Meyer H D, Manthe U and Cederbaum L S 1990 *Chem. Phys. Lett.* **165** 73
[20] Meyer H D, Manthe U and Cederbaum L S 1992 *J. Chem. Phys.* **97** 3199
[21] Beck M H, Jackle A, Worth G A and Meyer H D 2000 *Physics Reports* **324** 1
[22] Szabo A and Ostlund N S 1996 *Modern Quantum Chemistry* (New York: McGraw-Hill Inc.) Chapter 2
[23] Werner H J, Konwles P J, Amos R D, Berning A, Cooper D L, Deegan M, Dobbyn A J, Eckert F, Hampel C, Leininger T, Lindh R, Lloyd A W, Meyer W, Mura M E, Nickla A, Palmieri P, Peterson K, Pitzer R, Pulay P, Rauhut G, Schfltz M, Stoll H, Stone A J and Thoresteinsson T, MOLPRO A Package of *ab initio* Programs
[24] Schmidt M W, Baldridge K K, Boatz J A, Elbert S T, Gordon M S, Jensen J, Koseki S, Matsunaga N, Nguyen K, Su S, Windus T L, Dupuis M and Montgomery J A 1993 *J. Comput. Chem.* **14** 1347
[25] Fernandez R, Lopez R, Aguado A, Ema I and Ramirez G 1998 *J. Comput. Chem.* **19** 1284
[26] Fernandez R, Lopez R, Aguado A, Ema I and Ramirez G 2001 *Int. J. Quantum Chem.* **81** 148
[27] Birkeland T, Nepstad R and F?rre M 2010 *Phys. Rev. Lett.* **104** 163002
[28] Pindzola M S, Robicheaux F and Gavras P 1997 *Phys. Rev. A* **55** 1307
[29] Grobe R and Eberly J H 1994 *Phys. Rev. A* **48** 4664
[30] Hu S X, Collins L A and Schneider B I 2009 *Phys. Rev. A* **80** 023426